

# Neutron Depolarization Measurement by Using Pulsed Polarized Neutrons

Yasuo Endoh

*Department of Physics, Graduate School of Science, Tohoku University Aramaki Aza Aoba, Aoba-ku,  
 Sendai, 980-77 Japan*

(Received 15 May 1996; accepted 7 June 1996)

Recent research activities on the wave-length dependent depolarization studies on the mesoscopic magnetism carried out at the pulsed neutron scattering facility, KENS at KEK are reviewed.

KEYWORDS: Polarized neutrons, depolarization, pulsed neutrons, mesoscopic magnetism

## §.1. Introduction

In the past decade, we have developed the neutron wave-length dependent depolarization method<sup>1,2)</sup> and the instrumentation of this method.<sup>3)</sup> We also investigated the mesoscopic magnetism, which defines the study of the spatial magnetic disturbance with semi-macroscopic scale in spin glass, magnetic colloid, magnetic fluxoid in the superconductors, etc. This method does give a semi-quantitative determination of the scale of the magnetic structure, such as the coherence length and domain size, uniquely. It is very convenient to study temperature evolution of the magnetic disturbance in mesoscopic scale, which is difficult to study by the conventional diffraction technique, even by the conventional small angle scattering method.

Therefore as emphasized in the presentation, the depolarization method gives rise to a unique tool for the subtle problem of the spin glass transition, which is always difficult to answer from a unique experiment. We focus further discussion on this point rather than describing how the neutron depolarization technique works in general.

## §.2. Wave-length dependent depolarization method<sup>4)</sup>

First, we briefly describe the essence of the wave-length dependent depolarization method. This particular experimental method is the measurement of dephasing of the polarization of transmitted neutron beam through the magnetic medium. Since we can manipulate polychromatic polarized neutron beam as the pulse, we can measure the time dependent feature of depolarization which is then converted to the neutron wave-length dependence. Let me start to describe how the neutron polarization is depolarized. When we define  $\psi$  as the neutron wave function,  $\psi$  follows the equation of motion in the applied magnetic field,  $H$ .

$$i\hbar \frac{\partial}{\partial t} \Psi(t) = -\mu H \Psi(t) \quad (1)$$

Here  $\mu$  is the neutron magnetic moment, which is defined as  $\mu = \mu\sigma$ ,  $\sigma$  is the Pauli matrix. What we measure in the depolarization experiment is the neutron polarization,  $P$ , given by the eq.(5). To derive it, we follow the spin part of the neutron wave function, either  $\psi^+$  or  $\psi^-$ . We rewrite the eq.(1) and integrate as follows.

$$i\hbar \frac{\partial}{\partial t} \begin{pmatrix} \Psi^+ \\ \Psi^- \end{pmatrix} = -\mu \begin{pmatrix} H^z & H^- \\ H^+ & -H^z \end{pmatrix} \begin{pmatrix} \Psi^+ \\ \Psi^- \end{pmatrix}$$

$$\begin{pmatrix} \Psi^+(t) \\ \Psi^-(t) \end{pmatrix} = \frac{1}{H} A \begin{pmatrix} \Psi^+ \\ \Psi^- \end{pmatrix},$$

$$A = \begin{pmatrix} H \cos \omega t + iH^z \sin \omega t & iH^- \sin \omega t \\ iH^+ \sin \omega t & H \cos \omega t - iH^z \sin \omega t \end{pmatrix}. \quad (2)$$

Here  $\omega$  is the angular frequency of the neutron Larmor precession. If the initial polarization is perfect,

$$\begin{pmatrix} \Psi^+(0) \\ \Psi^-(0) \end{pmatrix} = \begin{pmatrix} 1 \\ 0 \end{pmatrix}, \quad (3)$$

the measured polarization is directly proportional to the depolarization matrix as in the following expression.

$$\begin{pmatrix} \Psi^+(t) \\ \Psi^-(t) \end{pmatrix} = \begin{pmatrix} H \cos \omega t + iH^z \sin \omega t \\ iH^+ \sin \omega t \end{pmatrix}. \quad (4)$$

The local magnetic field  $H$  generally has azimuthal angle  $\theta$  with respect to the neutron polarization axis,  $z$ . Then  $P^z(t)$  is given as a function of  $\theta$ .

$$P^z(t) = |\Psi^+(t)|^2 - |\Psi^-(t)|^2$$

$$= \frac{H^z^2}{H^2} + \frac{H^{x^2} + H^{y^2}}{H^2} \cos 2\omega t, \quad (5)$$

$$P^z(t) = \cos^2 \theta + \sin^2 \theta \cdot \cos 2\omega t. \quad (6)$$

Time dependence is then transformed to the neutron wave-length dependence by using the following relation.

$$t = \frac{L}{v} = \frac{Lm}{2\pi\hbar} \lambda, \quad (7)$$

$$P^z(\lambda) = \cos^2 \theta + \sin^2 \theta \cdot \cos(cLH\lambda), \quad (8)$$

$$c = \frac{\mu m}{\pi\hbar^2} = 4.63 \times 10^6 \text{ cm}^{-2} \cdot \text{Oe}^{-1}. \quad (9)$$

The major interest in our studies is not the effect of the Larmor precession in the stationary magnetic field but more complicated or inhomogeneous distribution of the local

field,  $F_H$ , in the magnetic media, where the length scale characterizing the inhomogeneity of the field is semi macroscopic or mesoscopic.

Nevertheless  $F_H$  is related to  $P(\lambda)$  as follows.

$$P(\lambda) = \int_0^\infty \int_0^\pi \int_0^{2\pi} P^z(\lambda) F_{H,\theta,\phi} dH d\theta d\phi, \quad (10)$$

$$P(\lambda) = 1 - a + a \int_0^\infty \cos(cLH\lambda) dH \quad (11)$$

$$a = \int_0^\pi \sin^2 F_\theta(\theta) d\theta.$$

The magnetic distribution function,  $F_H$ , can be derived by the Fourier transform of the above equation.

$$F_H = \frac{2cL}{\pi} \int_0^\infty \left[ 1 + \frac{P(\lambda) - 1}{a} \right] \cos(cLh\lambda) d\lambda$$

$$\frac{d}{d\lambda} P(\lambda) = -acL \int_0^\infty \sin(cLh\lambda) F_H H dH. \quad (12)$$

$$F_H = \frac{2}{a\pi h} \int_0^\infty \left[ \frac{d}{d\lambda'} P(\lambda') \right]_\lambda \sin(cLh\lambda) d\lambda$$

The last equation is therefore given as the general expression of the magnetic field distribution derived from the wave-length dependent neutron depolarization,  $P(\lambda)$ . However, this general form can not give a deep physical insight by itself. Moreover our analysis was restricted to be a component parallel to  $z$ , which limits a full depolarization information. Therefore we have studied some representative cases of the inhomogeneous field or the magnetic distribution,  $F_H$ , and derived an approximate form which are seen in our previous publications.<sup>1,2,4)</sup>

In next section, we present two kinds of typical experimental results of neutron depolarization measurements. Then physics taken out from the results will also be discussed.

### §.3. Experimental results

According to the eq.(11) the simpler case of the Gaussian distribution of  $F_H$  gives the following  $P(\lambda)$ , which has been further analyzed by fitting the wave-length dependent data.<sup>4)</sup>

$$P(\lambda) = P_0 + A \exp(-\sigma_I \lambda^2) \cos(I\lambda + \phi). \quad (13)$$

$\sigma_I$  and  $I$  represent, respectively, the distribution of the field inside the magnetized sample and the field integrated value throughout neutron pathlength. Here the stray magnetic field just outside of the magnetized samples causes the phase shift,  $\phi$ , as well as the deviation of the sum rule,  $P_0 + A = 1$ .

The eq.(13) could be utilized to most of the depolarization measurements for our investigation of the ferromagnetic domain distribution or the technical magnetization process.<sup>4)</sup> In this presentation, however, we show the result of the reentrant spin glass studies from  $\text{Fe}_{1-x}\text{Al}_x$  and  $\text{Fe}_x\text{Au}_{1-x}$  alloys. Let me start to explain the reentrant spin glass feature in the  $\text{Fe}_{0.715}\text{Al}_{0.285}$  alloy.<sup>5)</sup> At low temperatures below the reentrant transition

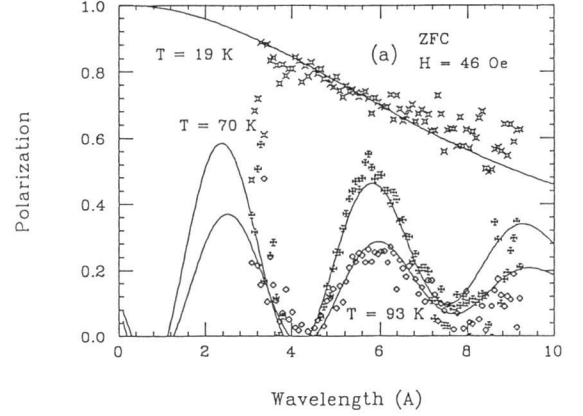


Fig. 1. Neutron wave-length dependence of  $\text{Fe}_{0.715}\text{Al}_{0.285}$  reentrant spin glass alloy of zero field cooling process (ZFC). Depolarization was measured under 40Oe. Two representative curves measured at 19K and 70K show the qualitative difference between Gaussian form in polarization and oscillatory function with respect to wave-length.

temperature,  $T_g = 68\text{K}$ , the data of  $P(\lambda)$  shows the qualitative difference between at  $T = 70\text{K}$  just above  $T_g$  and at  $19\text{K}$  well below  $T_g$  for the zero field cooling (ZFC) sample, as shown in Fig.1. The  $P(\lambda)$  curve at  $T = 19\text{K}$  is fitted to a simple Gaussian with  $I$  and  $\phi = 0$  at  $19\text{K}$ . On the other hand, the data of  $70\text{K}$  show the oscillation with respect to neutron wave-length, indicating the remanent magnetization in the sample. Note that the curve cannot be fitted to the eq.(13) in a certain temperature range below  $T_g$ . This fact obviously shows that the spontaneous magnetization diminishes at  $T_g$  upon cooling the sample in zero field. It indicates the reentrant spin glass transition. In this way, we could measure the thermal evolution of the reentrant spin glass behavior. The curve fitting of the wave-length dependent feature to the eq.(13) yielded the determination of parameters of  $P_0$ ,  $\sigma_I$  and  $I$ , which is plotted with respect to temperature in a range where  $T$  crosses  $T_g$ , which is seen in Fig.2(b). We emphasize here that, although thermal evolution of the magnetic susceptibility looks similar in two representative reentrant spin glass materials of  $\text{Au}_{1-x}\text{Fe}_x$ <sup>6)</sup> and  $\text{Fe}_{1-x}\text{Al}_x$  system,<sup>5,7)</sup> the wave-length dependent depolarization is apparently different as shown in Fig.2(a). However the difference arises in the concomitant parameters determining the depolarization, which might be related to the spatial scale factor characterizing the magnetic disturbance or the region of the spontaneous magnetic domain size as emphasized in the previous papers.<sup>1,6)</sup> For instance, we proposed a model of the inhomogeneous magnetic structure in the reentrant spin glass state for two examples as depicted in the schematic drawing of Fig.3.

Since then, more experiments have been conducted from different spin glass systems and this method is now recognized to be a unique tool for determination, for instance, of the spin glass transition.<sup>8-12)</sup>

Another example of the application of the wavelength dependent depolarization is investigation of the magnetic state in the type II superconductors.<sup>2,13,14)</sup> So far any of the

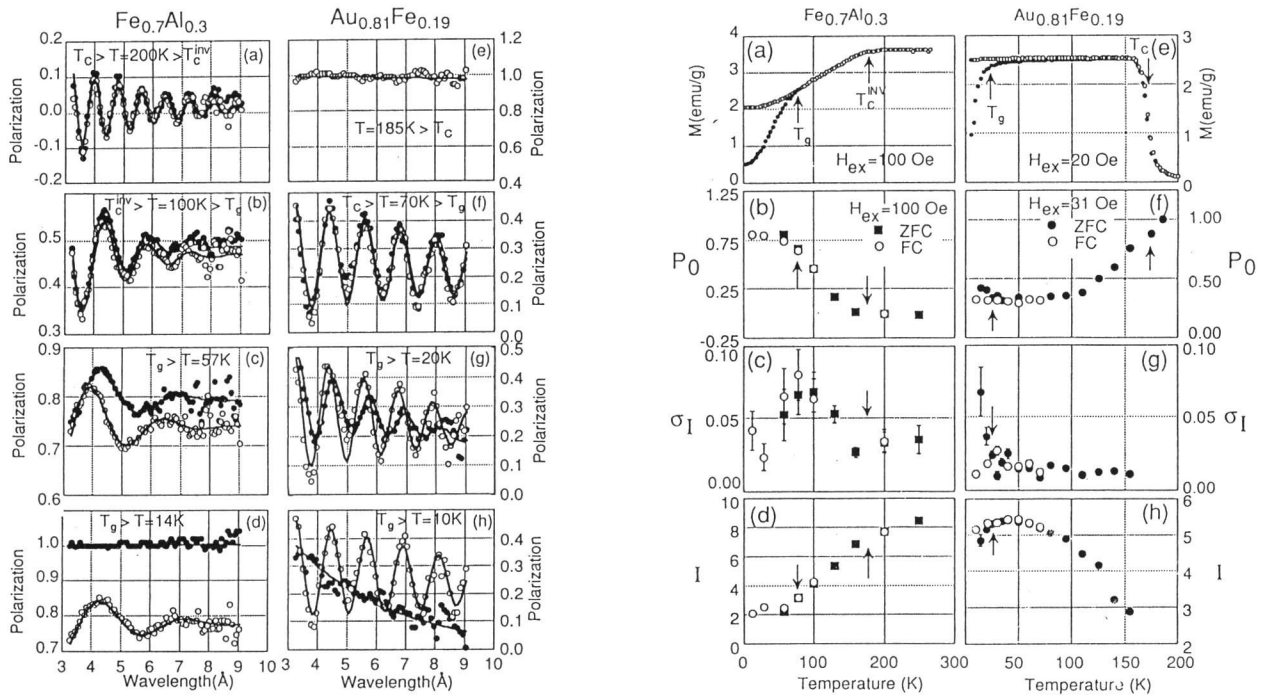


Fig. 2. Neutron depolarization from  $\text{Fe}_{0.7}\text{Al}_{0.3}$  and  $\text{Au}_{0.81}\text{Fe}_{0.19}$  reentrant spin glass alloy. (a) wave-length dependence of neutron polarization at several designated temperatures. Open and closed marks represent FC and ZFC processes respectively. (b) Temperature dependence of the fitted parameters of Eq.(13).

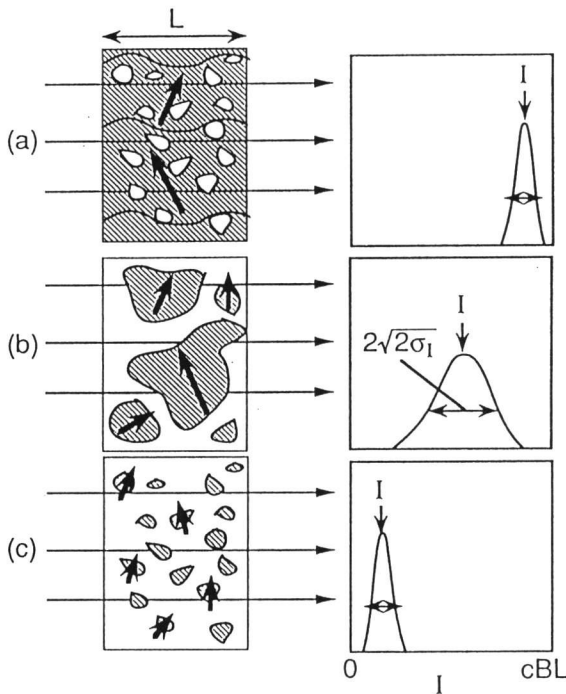


Fig. 3. Schematic drawing of neutron passage through the sample of typical reentrant spin glass phase. Shaded and white areas represent the ferromagnetic domain and spin glass area, respectively. Arrows are the local magnetization of each domain. Magnetic field integral is shown in the right hand side of each phase of (a) at  $T_{inv} > T > T_g$ , (b) at  $T \approx T_g$ , or (c) at  $T_g > T$ .

measurement of the magnetic flux distribution in such superconducting substances is restricted to be the surface probe such as the decoration method, STM or even the LEED measurement. This simple measurement of the depolarization of the transmitted beam probes the magnetic field inside the bulk like the  $\mu\text{SR}$  or neutron diffraction at the small angle scattering and therefore it gives potentially very useful information: whether the magnetic flux penetrates through the bulk superconductor and/or the determination of the flux penetration depth. Since the details of the depolarization measurement of the magnetic flux determination is described separately,<sup>14)</sup> thermal evolution of the depolarization from the field-cooled high temperature superconductor is presented and the result is discussed in terms of the currently developed flux lattice melting picture.

Single crystals of flat disk shape were cut from the bulky boule grown in our group,<sup>15)</sup> typically 5 mm in diameter and 3 mm thick. Either the crystalline  $c$  axis is oriented normal to the disk or lies in the disk plate. The field cooling magnetic field ( $H_c$ ) is always applied in the disk plate so that the magnetic flux is embedded along the field direction during the FC process. The samples were prepared by choosing  $H_c \parallel c$  or  $H_c \parallel a$ . The geometrical configuration for the depolarization is following. The neutron polarization,  $P$ , was kept vertically by applying the weak homogeneous field, which was perpendicular to the direction of neutron track. Since  $P$  was also fixed to be perpendicular to  $H_c$  and hence  $P \perp H_c$ ,  $P$  should rotate around the magnetic flux and then the oscillatory wave length dependence of the polarization of the transmitted neutrons should be observed, if the magnetic fluxes are pinned along  $H_c$ , as shown in the illustration of Fig.4.

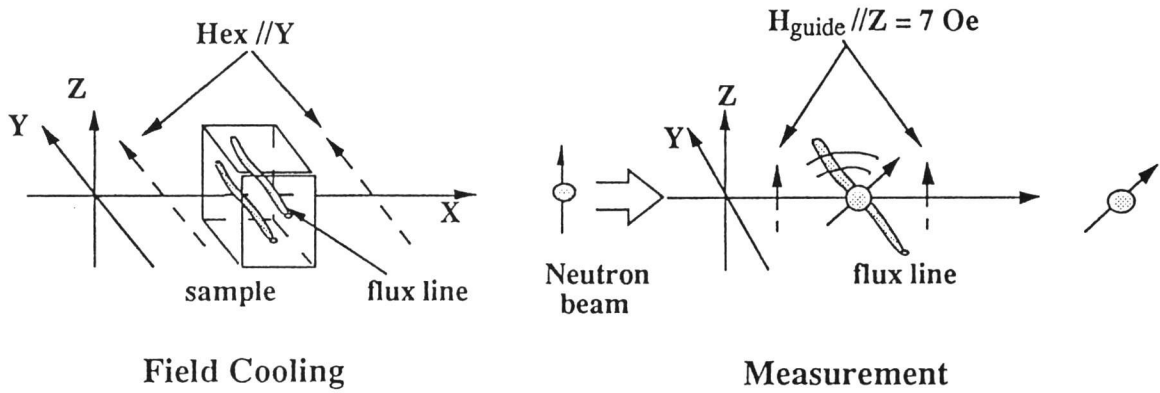


Fig. 4. Schematic drawing of the experimental configuration of detection of the magnetic fluxes in the superconductor. The way to embed the magnetic flux by field cooling with the external field of  $H_{ex}$  is shown at right. X directs the neutron track. Depolarization is measured with the configuration shown at left. Neutron polarization is represented by arrow mark.

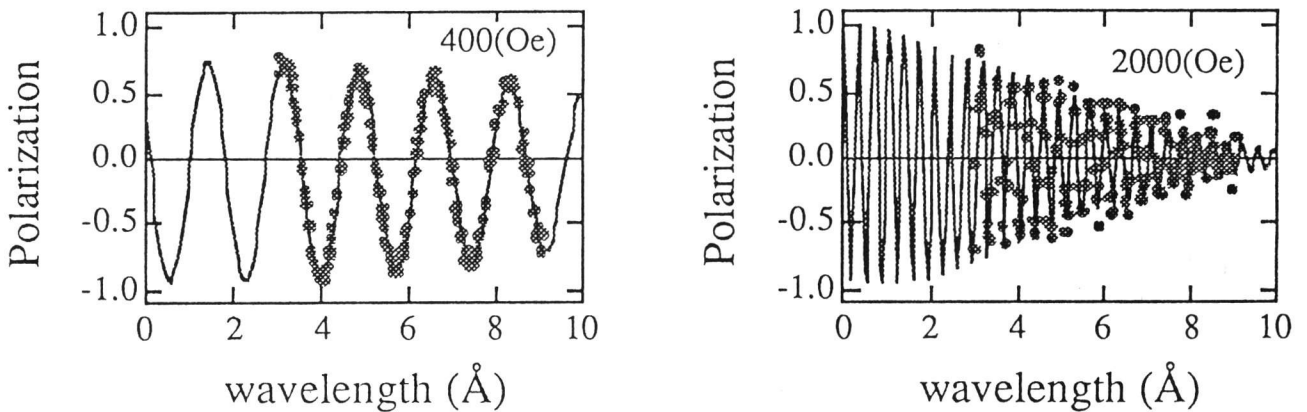


Fig. 5. Oscillatory function with the decay of the polarization envelope against neutron wave-length at 400Oe and 2000Oe FC processes respectively.

In fact, the oscillation behavior was clearly observed with the amplitude of the polarization, which decreases with increase of the neutron wave-length as shown in Fig.5. The result immediately indicates the existence of the nonuniform magnetic field distribution in the bulk of the superconductor. In fact this crystal shows the superconducting transition at 37.3K. It is therefore a direct evidence of the formation of the magnetic flux lattice at low temperatures under the moderate magnetic field. From the period of the oscillation with respect to neutron wave-length as well as the envelop curve of the amplitude oscillation of the polarization,  $I$  and  $\sigma$  are deduced by fitting the curve to Eq.(13). Then these quantities were further analyzed by using the simple model of the uniform vortex lattice model. The flux density in the bulk and the penetration depth were determined as well, which is given in the separate paper.<sup>14)</sup>

To emphasize a unique evidence obtained for the first time, the oscillatory behavior is reported to remain in the region where the remanent magnetization disappears in the magnetization data measured by a SQUID susceptometer in the high temperature superconductor.<sup>14)</sup> In other words, the magnetization measured by the depolarization experiment shows a finite value of the remanent magnetic field in the bulk in a region near  $T_c$ , where the bulk

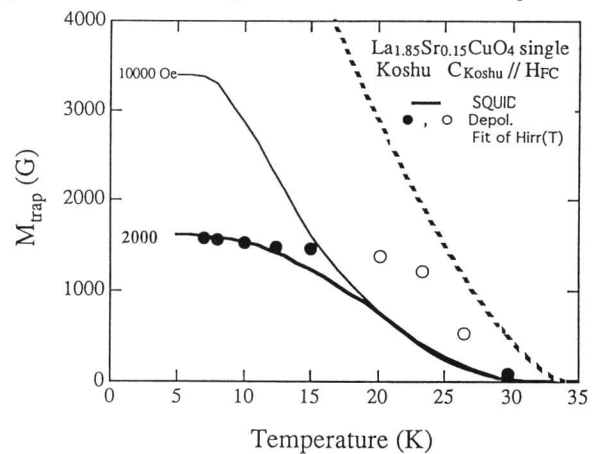


Fig. 6. Magnetic field extracted from the depolarization measurement with 2000Oe field cooling process ( $H_d/c$ ) of  $\text{La}_{1.85}\text{Sr}_{0.15}\text{CuO}_4$  single crystal ( $T_c=33\text{K}$ ) measured at several temperatures below  $T_c$ . Circles indicate the results of depolarization measurements and solid lines are SQUID measurements. Dot line represents the irreversible line for this crystal.

magnetization reaches zero by the susceptibility measurement, which is shown in Fig.6. Before this experiment was presented, there had been no definite evidence showing the entangled flux state, as far as I know. This result is not an experimental error, nor a trivial effect, because the remanent magnetization by the depolarization

measurement perfectly coincides with those of susceptibility measurement from the  $V_3Si$  single crystal, of the typical type II superconductor. The depolarization can probe the net magnetic field in the sample, but the magnetization measurement under the DC applied field detects only the field component. Therefore the simplest interpretation of the discrepant results arises in the different magnetization quantities of these different methods. In this case, the experimental result suggests that the magnetic fluxes embedded in the high  $T_c$  superconductor might be entangled or at least the magnetic flux lattice might be significantly disordered as temperature and the applied field approach to the boundary of the  $H_{c2}$  line. It should be noted that the data points of the remanent magnetization determined by the depolarization measurement almost coincide with a critical line of the irreversible field even in this unusual superconductor. Nevertheless the present result indicates the existence of the melting of the fluxoid.

To conclude, the wave-length dependent depolarization measurement shown here demonstrates a unique tool for the study of the meso-scopic magnetism. We comment here that in order to make the depolarization method stronger, we should implement a neat device controlling the neutron polarization perfectly just outside of the magnetized sample, like the zero field polaritometry proposed by Tasset.<sup>16)</sup> We also consider the three dimensional depolarization analysis and thus we propose such an advanced depolarization instrument equipped with the full options, when a new generation pulsed neutron facility of JHP is realized in the future.

#### Acknowledgments

The presentation is based on the recent activities of our group to develop the first generation depolarization instrument and a new experimental method of the neutron wave-length dependent depolarization at the spallation pulsed neutron facility at KEK. The author thanks his past students of S. Mitsuda, S. Itoh, T. Watanabe and J. Suzuki for their enthusiastic experimental efforts and joyable discussions. The work was supported by a Monbusho Grant-in-Aid for the Scientific Research and a SAT Grant for the Promotion of Science.

- 1) Y. Endoh: *Prog. Theor. Phys. Suppl.* 101 (1990) 567.
- 2) Y. Endoh, S. Itoh, T. Watanabe and S. Itoh: *Physica B* 180&181 (1992) 34.
- 3) Y. Endoh, S. Ikeda, S. Mitsuda and H. Fujimoto: *Nucl. Instrum. & Methods, A* 240 (1985) 115.
- 4) S. Mitsuda and Y. Endoh: *J. Phys. Soc. Jpn.* 54 (1985) 1570.
- 5) J. Suzuki, Y. Endoh, M. Arai, M. Furusaka, H. Yoshizawa: *J. Phys. Soc. Jpn.* 59 (1990) 718.
- 6) S. Mitsuda, H. Yoshizawa, T. Watanabe, S. Itoh, Y. Endoh and I. Mirebeau: *J. Phys. Soc. Jpn.* 60 (1991) 1721.
- 7) S. Mitsuda, H. Yoshizawa and Y. Endoh: *Phys. Rev. B* 17 (1992) 9788.
- 8) I. Mirebeau, S. Itoh, S. Mitsuda, T. Watanabe, Y. Endoh, M. Hennion and R. Papoular: *Phys. Rev. B* 41 (1990) 11405.
- 9) I. Mirebeau, S. Itoh, S. Mitsuda, T. Watanabe, Y. Endoh, M. Hennion and P. Calmettes: *Phys. Rev. B* 44 (1991) 1013.
- 10) T. Sato, T. Ando, T. Watanabe, S. Itoh and Y. Endoh: *J. Magn. Magn. Mater.* 104-107 (1992) 1625.
- 11) I. Mirebeau, M. Hennion, S. Mitsuda and Y. Endoh: in *Recent Progress in Random Magnets* ed by D.H. Rhan, pp41, (World Scientific, Singapore, 1992)
- 12) T. Sato, T. Ando, T. Watanabe, Y. Endoh, M. Furusaka: *Phys. Rev. B* 48 (1993) 6074.
- 13) Y. Endoh, T. Watanabe, K. Yamada, S. Itoh, I. Tanaka and H. Kojima: *Physica C* 185-189 (1991) 1839.
- 14) T. Watanabe and Y. Endoh: unpublished
- 15) S. Hosoya, C.H. Lee, S. Wakimoto, K. Yamada and Y. Endoh: *Physica C* 235-240 (1994) 547.
- 16) V. Nunes, P.J. Brown, T. Chattopadhyay, J.B. Forsyth and F. Tasset: *Physica B* 180-181 (1992) 903.